Title	Application of broadband acoustic resonance dissolution spectroscopy (BARDS) to the gas release behaviour during rehydration of milk protein isolate agglomerates
Authors	Wu, Shaozong;Fitzpatrick, John;Cronin, Kevin;Ahmed, M. Rizwan;Fitzpatrick, Dara;Miao, Song
Publication date	2019
Original Citation	Wu, S., Fitzpatrick, J., Cronin, K., Ahmed, M. R., Fitzpatrick, D. and Miao, S. (2019) 'Application of broadband acoustic resonance dissolution spectroscopy (BARDS) to the gas release behaviour during rehydration of milk protein isolate agglomerates', Journal of Food Engineering, 253, pp.14-20. https://doi.org/10.1016/j.jfoodeng.2019.02.010
Type of publication	Article (peer-reviewed)
Link to publisher's version	https://doi.org/10.1016/j.jfoodeng.2019.02.010
Rights	© 2019, Elsevier Ltd. All rights reserved. This manuscript version is made available under the CC BY-NC-ND 4.0 license. - https://creativecommons.org/licenses/by-nc-nd/4.0/
Download date	2024-05-28 00:10:53
Item downloaded from	https://hdl.handle.net/10468/15602

Accepted Manuscript

Application of broadband acoustic resonance dissolution spectroscopy (BARDS) to the gas release behaviour during rehydration of milk protein isolate agglomerates

Shaozong Wu, John Fitzpatrick, Kevin Cronin, M. Rizwan Ahmed, Dara Fitzpatrick, Song Miao

PII: S0260-8774(19)30056-1

DOI: https://doi.org/10.1016/j.jfoodeng.2019.02.010

Reference: JFOE 9526

To appear in: *Journal of Food Engineering*

Received Date: 21 November 2018

Revised Date: 8 February 2019

Accepted Date: 11 February 2019

Please cite this article as: Wu, S., Fitzpatrick, J., Cronin, K., Ahmed, M.R., Fitzpatrick, D., Miao, S., Application of broadband acoustic resonance dissolution spectroscopy (BARDS) to the gas release behaviour during rehydration of milk protein isolate agglomerates, *Journal of Food Engineering* (2019), doi: https://doi.org/10.1016/j.jfoodeng.2019.02.010.

Application of broadband acoustic resonance dissolution spectroscopy (BARDS) to the gas release behaviour during rehydration of milk protein isolate agglomerates

Shaozong Wu[a,b], John Fitzpatrick[b], Kevin Cronin[b], M.Rizwan Ahmed[c], Dara Fitzpatrick[c], Song Miao[a,*]

[a] Teagasc Food Research Centre, Moorepark, Fermoy, Co. Cork, Ireland

[b] Process & Chemical Engineering, School of Engineering, University College Cork, Cork, Ireland

[c] Department of Chemistry, Analytical and Biological Chemistry Research Facility (ABCRF), University College Cork, Cork, Ireland* Correspondence: song.miao@teagasc.ie; Tel.: +353-(0)-25-42468

Abstract

The BARDS technique was applied in this study to acoustically assess the rehydration behaviour of milk protein isolate (MPI) agglomerates and to compare with regular MPI powder. The results showed that BARDS has potential to monitor the rehydration behaviour of agglomerates. The greater porosity (> 70%) of agglomerated powders introduced more compressible gas into the water. The BARDS profile showed that there was faster initial gas release from the agglomerates, indicating better wetting and dispersion ability of the agglomerates with shorter t_M (time of maximum gas volume in solution). At 0.10% powder addition, agglomerated MPI reached t_M within 109 s, which was significantly less than the control MPI at 140 s. MPI with lactose binder (MPI-L) had a t_M of 80 s at 0.10% powder addition and, larger size MPI-L had a t_M of 60 s. At 0.20% and 0.30% powder addition, more time was required to wet and disperse the powders.

Key words: BARDS, milk protein isolate powder, rehydration, agglomeration

1. Introduction

Fluid-bed agglomeration is a technique that binds primary particles together to form aggregates with larger particle size. It can be applied to improve the physical properties of powders such as flowability and rehydration ability (Chever et al., 2017), and is used widely in the food industry. MPI (milk protein isolate) powder is an important product produced by the dairy industry, and is used as a milk protein ingredient in many food products. A major problem with MPI powder is its rehydration ability (Fitzpatrick et al., 2016). It is both a poor wetting and slowly dissolving powder (Crowley et al., 2015; Ji et al., 2015; Wu et al., 2019). The high content of casein present in MPI powder is considered as the major reason for its slow dissolution (Mimouni et al., 2010). Crowley et al. (2015) characterised the rehydration ability of milk protein concentrate (MPC) powders with milk protein concentrations ranging from 35 to 90%. They showed that increasing protein content reduced powder wettability. It also reduced powder dissolution ability especially at protein contents of 70% and higher. Ji et al (2015) showed that fluid-bed agglomeration could greatly improve the wettability of MPI powder, as the larger agglomerate particle size made it easier for water to penetrate the interstitial spaces between the particles. However, it did not improve the speed of dissolution of the particles once they were wetted and dispersed. In fact, agglomeration caused the dissolution to be slightly slower because a short period of time was required to break-up the agglomerate structure into the primary particles, which then dissolved slowly like in the regular MPI powder.

The dissolution process of powder in principle includes the gas exchange between powder and solution, that is, the gas inside the powder particles is released into the water as water penetrates into the particles and dissolves the powder material. However, the literature mainly focuses on the dissolution of material in powder form (Felix da Silva et al., 2018). Furthermore, when powder is re-structured by agglomeration, the air distribution in the powder is inevitably altered. The air release behaviour of agglomerated powder during rehydration is rarely discussed even though this can potentially provide important insights into the rehydration process.

Broadband acoustic resonance dissolution spectroscopy (BARDS) is a technique that can monitor gas release from powder in solution. The gas release has response in the acoustic resonance, which is influenced by the changes in the medium due to the release of air bubbles into the solvent during powder dissolution. The frequency change of BARDS results from the alteration of the speed of sound in the solvent containing air bubbles. Hence, the real-time information in the solvent can be monitored acoustically by changes in frequency (Fitzpatrick et al., 2014). So theoretically, the rehydration process of a dissolving powder can be described acoustically by BARDS. The first application of BARDS to the rehydration of dairy powder was reported for MPC powders with protein contents ranging from 35 to 90% (Vos et al., 2016). Rehydration of the different MPCs was monitored using BARDS, from which their rehydration characteristics were acoustically distinguished. The higher protein content powders showed slower gas release, which is indicative of slower rehydration behaviour. (Peddapatla et al., 2017) applied BARDS to investigate the wettability of pharmaceutical blends. Very poor wetting blends did not disperse into water and thus there was no gas release, while good wetting blends

70 readily dispersed and dissolved, releasing air bubbles that altered the frequency
71 response measured by BARDS.

72 The objective of this study is to apply the BARDS technique for investigating the
73 gas release of fluid-bed agglomerated MPI powders during rehydration and to
74 compare this behaviour with that of regular unagglomerated MPI powder.
75 Agglomeration of MPI was achieved using both water and lactose solution as binders
76 to investigate the influence of binder type. The agglomerated MPI was sieved into
77 two size fractions to investigate the influence of agglomerate particle size.

78

79 **2. Materials and methods**

80 **2.1. Materials**

81 Milk protein isolate (MPI) powder was purchased from Kerry Ingredients (Country
82 Kerry, Ireland). The solids composition of the MPI powder is 86% protein, 1.5 % fat,
83 6% ash and <1 % carbohydrate. Crystalline lactose powder was supplied by Arla
84 Food Ingredients (Viby J, Aarhus, Denmark).

85 **2.2. Powder preparation**

86 The agglomerated MPI was prepared in a top-spray fluidised bed granulator (VFC-
87 Lab Micro flo-coater, Vector Corporation, Lowa, USA). The quantity of MPI produced
88 in each trial was 100 g. The volume of binder solution was 50 mL, and this was
89 transferred by a peristaltic pump at a flowrate of 1.2 $mL \cdot min^{-1}$. The powder was
90 fluidised in the bottom of the chamber by air at 50°C, while the binder was sprayed
91 through a nozzle with a 1 bar pressure drop. After agglomeration, the powder was
92 dried for 15 minutes by the air at 50°C. MPI agglomerates were produced using two

binders, one being water (MPI-W) and the other being a 15%, w/v lactose solution (MPI-L). Both MPI agglomerates were sieved to produce two size fractions with particle sizes between 106 and 180 μm and 180 and 300 μm.

2.3. Physical properties of powder

2.3.1. Particle size

Malvern Morphologi G3 (Malvern Instruments Ltd, Worcestershire, UK) was used to characterize the particle size distribution. A 15 mm^3 volume of powder was dispersed by air as a single layer of powder on a glass plate in the dispersion unit. The Morphologi G3 measured the number size distribution from which the volume size distribution was evaluated, along with corresponding D_{10}, D_{50}, and D_{90} values. The experiment was performed in duplicate for each size distribution.

2.3.2. Density and gas volume

The loose bulk density (ρ_B) and tapped bulk density (ρ_T) of the MPI powder and its agglomerates were measured using a measuring cylinder and a tapping machine (Ji et al., 2015). The powder was tapped 500 times by the tapping machine (Funke Gerber, Berlin, Germany). The apparent density (ρ_A) was measured by a helium gas pycnometer (AccuPyc II 1340, Micromeritics Instrument Corporation, Georgia, USA). The measurements were done in triplicate. The solid density (ρ_S) of MPI and MPI-W was 1.53 g/mL, while the MPI-L was 1.54 g/mL. These were evaluated using the composition of MPI and its agglomerates (Niro, 2006).

In the MPI powder and its agglomerates, there are a number of void spaces where air resides, as illustrated in Fig. 1. In the MPI powder, there are vacuoles within the powder particles and interstitial air between powder particles in the bulk. A fluid-bed

agglomerate particle consists of primary particles bound together, thus there is additional vacuole space between the primary MPI particles within the agglomerate particle.

The porosity of the MPI powder and its agglomerates is defined in equation (1).

$$\mathcal{E} = (\rho_A - \rho_T)/\rho_A \times 100 \quad (1)$$

For the MPI powder, this represents the void fraction associated with interstitial voids in the tapped powder and possibly some vacuole voids within the primary particles, but this does depend on whether or not the pycnometer gas penetrates inside the primary particles. For the MPI agglomerates, the porosity includes additional voidage associated with the voids between primary particles within the agglomerate particles, as these are easily penetrated by the pycnometer gas.

The following specific air volumes are defined using the density data. These are the bulk interstitial air (BIA), tapped occluded air (TOA) and vacuole occluded air (VOA) specific volumes. These are defined in equations (2) to (4), and they are expressed in units of mL / 100 g of powder.

$$BIA = \left(\frac{1}{\rho_B} - \frac{1}{\rho_T}\right) \quad (2)$$

$$TOA = \left(\frac{1}{\rho_T} - \frac{1}{\rho_A}\right) \quad (3)$$

$$VOA = \left(\frac{1}{\rho_A} - \frac{1}{\rho_S}\right) \quad (4)$$

Chever et al. (2017) and GEA Niro (Niro, 2006) use similar definitions to characterise specific air volumes in powder and agglomerates.

2.4. The measurement of BARDS

The BARDS apparatus consists of a rehydration vessel, which is a glass vessel with a magnetic stirring bar, and a microphone placed 5 cm above the top rim of the glass vessel. A known mass of powder is dropped onto the surface of the water in the glass vessel. The broadband acoustic excitation is obtained from the tapping behaviour of a magnetic bar on the inner glass wall. The microphone captures the acoustic resonance from the sound travelling through the liquid, typically in the frequency range of 0-20 kHz. The BARDS instrument was stabilized for 30 s to allow a steady-state frequency to be achieved before powder is added (Ahmed et al., 2018). Gas is released from the powder which alters the measured frequency as the powder wets and dissolves. The frequency decreases over time until it attains a minimum value (f_{min}), after which the frequency gradually returns to its original steady state value.

The volume of distilled water in the measuring vessel of BARDS was 25 mL. Three masses of each powder were used, that is 0.025 g, 0.0375 g and 0.05 g, giving powder concentrations in water of 0.1%, 0.15% and 0.2% w/v, respectively. The duration of the BARDS measurement was recorded over an 800 s duration and each test was carried out in duplicate. The stirring rate was 500 rpm in ambient temperature. The small masses of powder readily wetted and dispersed. A typical frequency profile over time is presented in Fig. 2. As stated above, the essence of the BARDS measurement technique is that as a powder dissolves in a liquid, it releases its entrained air to the (already saturated) liquid in the form of micro-bubbles and this correspondingly affects the frequency of sound in the liquid. The relationship between the frequency response and the fractional volume occupied by

the air bubbles is presented in equation (5), and details of this equation are provided by Fitzpatrick et al. (2012) and Crawford (1982).

$$freq=\frac{freq_w}{\sqrt{1+1.49\times10^4\cdot f_a}} \quad (5)$$

where f_a is the fractional volume occupied by air bubbles. The $freq_w$ and $freq$ are the frequency response of pure water in steady-state and bubble-filled water after adding sample, respectively. The equation and its parameter values are valid for the conditions prevailing for our work. The volume of gas (V_g) in the water in the BARDS glass vessel can be calculated from equation (6), where V_w is the volume of water for rehydrating powders in BARDS.

$$V_g = f_a \cdot V_w \quad (6)$$

2.5 Statistical analysis

One-way analysis of variance (ANOVA) was performed by SPSS software (IBM SPSS Statistics version 24). Duncan test was run for comparing the significance of multiple groups. The significance was set as $P<0.05$.

3. Results and discussion

3.1. Powder particle size, densities and specific gas volumes

Particle size values for the MPI powder and its agglomerates are presented in Table 1. As expected, the particle size of agglomerated powders is much larger than that of the non-agglomerated powder. The D[v, 0.5] value of the MPI powder is 49.8 μm. The D[v,0.5] values of the smaller size agglomerate fractions are 119 μm for

MPI-W1 and 117 µm µm for MPI-L1. The D[v,0.5] values of the larger size agglomerate fractions are 207 µm for MPI-W2 and 168 µm for MPI-L2. Powder agglomerated by water is larger than the powder agglomerated by lactose, especially for the larger size fractions. Jinapong et al. (2008) also observed that smaller sized soymilk agglomerates were obtained by increasing the concentration of maltodextrin binder from 0 to 10 %. Similarly, Szulc and Lenart (2013) showed that larger sized agglomerates were achieved using distilled water as the binder.

The powder densities of the MPI powder and its agglomerates are presented in Table 2. The apparent densities of the MPI powder and its agglomerates are all fairly similar with the agglomerates having slightly greater apparent densities ranging from 1082 to 1119 g/L, and the MPI having a value of 1073 g/L, which is in line with a study by (Szulc and Lenart, 2013). The similar apparent densities are to be expected as the fluid-bed agglomerates are composed of primary MPI particles, and the pycnometer gas will penetrate them to the same extent whether they are in the MPI powder or the MPI agglomerates. The solid bridges in the agglomerate are possibly the reason why the agglomerates have slightly greater apparent densities. Table 2 shows that both the loose and tapped bulk densities of the agglomerates are smaller than the MPI powder. This is to be expected because of the additional voids that exist between the primary particles within the agglomerate particles themselves. In relation to the agglomerates, the different particle size fractions showed different tapped bulk densities, with the smaller size fractions having larger tapped bulk densities.

The porosity of the powders was calculated in equation (1), using the apparent density and tapped bulk density. The porosity of the MPI powder and its agglomerates are presented in Table 2. The porosity of the agglomerates is greater

than that of the MPI powder, due to their lower tapped bulk densities as highlighted above. Likewise, the porosity of the larger sized agglomerates was significantly greater than the smaller sized agglomerates, while the type of binder had little effect on porosity.

The BIA, TOA and VOA specific volumes (equations 2-4) are presented in Table 3 for the MPI powder and its agglomerates. The VOA had similar specific volumes in accordance with the apparent densities. This suggests that the pycnometer gas easily penetrates the porous structure between the primary particles in the agglomerates. The open pores in agglomeration possibly favour the gas penetration as well (Al hassn et al., 2018). Consequently, the VOA represents some or all of the specific air volume within the primary MPI particles, depending on the ability of pycnometer gas to penetrate into these particles. The VOA of primary MPI particle is probably dependent on the powder shrinkage during spray-drying (Foerster et al., 2016a; Foerster et al., 2016b; Fu et al., 2013). The TOA specific volumes have the same trend as porosity, with the agglomerates having larger TOA values than the MPI powder and the larger agglomerates have larger values than the smaller agglomerates. The TOA values represent the specific air volume between particles in the tapped bulk plus the specific air volume within the structure of the agglomerates and possibly some air volume within the primary MPI particles (depending on the ability of pycnometer gas to penetrate into these particles). The BIA values represent the change in specific volume between the loose and tapped bulks.

3.2 BARDS profiles for MPI and agglomerated MPI

This section compares the behaviour of agglomerated and non-agglomerated MPI, by initially comparing the BARDS profile of the MPI powder with one of the agglomerates, i.e. MPI-W2, at 0.1% w/v concentration of powder in water. The effect of agglomerate particle size, binder type and powder concentration in water are considered in subsequent sections. The BARDS acoustic profiles for the MPI powder and MPI-W2 are presented in Fig. 3a. For both powders, the frequency initially decreases to a minimum value and then increases gradually back to the original steady-state frequency. The change in frequency during powder rehydration is due to the change of the volume of gas in the water. The gas volume in water was estimated from equations (5) and (6) using the BARDS frequency data. The gas volume profiles for MPI and its agglomerate are presented in Fig. 3b. This shows a greater volume of gas release for the MPI agglomerate, which is to be expected considering its porosity is greater than the MPI powder. During the test, gas is being generated as gas is transferred from the particles into the water, and gas is being eliminated as gas leaves the surface of the water at the top of the vessel. The up-slope (Fig. 3b) indicates that gas generation rate is greater than gas elimination rate, and vice-versa during the down-slope. The frequency minimum or gas volume maximum indicates where the two rates are equal.

The time (t_M) at which the maximum gas volume (or minimum frequency) occurs is indicative of the rehydration ability of the powder, with shorter times being indicative of faster or better rehydration ability (Peddapatla et al., 2017). Fig. 3 shows that the agglomerated MPI powder had a shorter t_M than the MPI powder. Table 4 shows that t_M for the agglomerated powder and MPI powder were 85 s and 140 s, respectively. After t_M, Fig. 3 shows that return trajectories towards steady-state became similar with similar return times of about 450 s.

Previous work in the research group, conducted by Ji et al. (2015), experimentally compared the rehydration behaviour of MPI and agglomerated MPI. The wetting and dissolution behaviour of MPI and MPI agglomerates were measured. The MPI agglomerates in this BARDS study were prepared using the same techniques as presented by Ji et al. (2015) and had similar sizes and used the same binders. Ji et al. (2015) showed that agglomeration improved the wetting ability of the powder because it was easier for water to penetrate into the spaces between the larger sized agglomerate powder. Consequently, the agglomerated powder particles wetted more quickly and the agglomerate structure broke down readily liberating the primary MPI particles. This concurs with the BARDS profiles whereby the quicker wetting leads to faster release of interstitial gas and the break-up of the agglomerate structure leading to the release of vacuole air between the primary particles within the agglomerate structure. This results in greater gas release and a shorter t_M, as illustrated in Fig. 3b. This figure also shows that the MPI and the MPI agglomerate have similar return trajectories to steady-state, with both attaining steady-state at about 450 s. This can be explained by the gradual dissolution of the primary MPI particles, which was experimentally shown by Ji et al. (2015). Once the agglomerates wet and disintegrate to release the primary MPI particles, which is rapid, the rehydration is rate-limited by the dissolution of the MPI primary particles.

3.3 Effect of particle size and binder

Table 4 shows that all the agglomerates have shorter t_M times than the MPI powder and this is consistent for all three concentrations, highlighting the better wetting behaviour of the agglomerates. This is in line with the effect of granulation on powder wetting (Schuck, 2009). Furthermore, the return to steady-state trajectories

of all the agglomerates and the MPI powders are similar, as illustrated in Figs. 4 and 5, which is indicative of the gradual dissolution of the MPI primary particles.

For the MPI agglomerates themselves, Table 4 shows that the larger sized agglomerates had shorter t_M times. This is due to faster wetting of larger sized particles, as water will penetrate more rapidly into the interstitial void spaces between the agglomerates. The faster wetting is also potentially due to the higher porosities (Table 2) and higher tapped occluded specific air volumes (Table 3) of the larger agglomerates. This may give rise to a more open porous structure within the larger agglomerates allowing water to penetrate more easily into the void spaces within the agglomerates and allowing gas to escape more rapidly. This is consistent with another study showing that large particles forming large pores and high porosity favour fast wetting (Gaiani et al., 2005). Furthermore, the effect of agglomerate size is consistent for all three concentrations.

The effect of the binder (water vs lactose solution) is also presented in Table 4. Shorter t_M times were obtained for lactose agglomerates containing the lactose binder. This occurs consistently at all three concentrations. The agglomerates with lactose and water binders have very similar porosities (Table 2), thus it is not a porosity effect. It is most likely because the lactose containing bridges are more hydrophilic (Li et al., 2016), which more rapidly dissolve resulting in easier break-up of agglomerates and release of air into the water. The presence of lactose can inhibit protein interaction and pave the way for water transfer within micelles during the rehydration process (Baldwin, 2010).

The trends presented by BARDS above are in line with work presented by Ji. et al. (2016), which also showed that larger agglomerate particle size and lactose binder

resulted in faster wetting. This shows that the BARDS technique is effective at assessing these effects on the rehydration behaviour of the MPI agglomerates.

3.4 Effect of concentration

As expected, Fig. 5 shows that there is more gas volume released by powder at higher concentrations of powder in water, simply because there is more powder present. Table 4 shows that there is a general trend that increasing the concentration of powder in water from 0.1% to 0.15% to 0.2% results in an increase in the t_M times for the MPI and all the MPI agglomerates. For example increasing the concentration from 0.1% to 0.2% resulted in t_M increasing from 140 s to 244 s for the MPI powder, and from 60 s to 80 s for the MPI-L2 powder. This is indicative of slower wetting at higher concentrations for all the powders, and shows that BARDS is effectively monitoring the influence of concentration. Furthermore, the return to steady-state took longer with increased concentrations, as illustrated in Figs. 4 and 5, with return times being about 450 s for the MPI powders and greater than 800 s for the higher concentrations. This is consistent with work conducted by Vos et al. (2016).

There are a number of reasons that potentially explain the effect of concentration on slowing the rehydration behaviour. The more powder that is added the longer it will take for all of the powder to wet and disperse, which is in agreement with a previous study (Fitzpatrick et al., 2014). A notable shift of time taken for the acoustic profiles returning to steady state from t_M was observed with more powder added. It will also result in more gas in the water which will take longer to be eliminated from the water. The more powder present will lead to more powder in solution which lowers the mass transfer driver and thus slows the rehydration process. The more powder present will also tend to increase viscosity which will slow the mass transfer

of water and gas between the particles and water, and slows the elimination of gas from the water.

4. Conclusion

BARDS is a promising technique for studying the rehydration behaviour of powders by measuring the gas release behaviour over time. In this work, it was shown that the BARDS technique could be applied for assessing the rehydration behaviour of MPI agglomerates. Their faster gas generation showed that the agglomerates wetted and dispersed more rapidly than the regular MPI powder. The similar return trajectories to steady-state showed and the dissolution behaviours of the agglomerates were similar to that of the MPI and were rate-limited by the slow dissolution of the MPI primary particles. The technique was able to distinguish the different wetting and rehydration behaviours of different size agglomerates and agglomerates formed with different binders, because these factors influence the rate at which the agglomerates are wetted and rate at which the agglomerate structure disintegrates and releases gas. Overall, the study has shown that BARDS is a convenient, easy to use technique that can be applied to study the rehydration behaviour of agglomerates and to compare with the non-agglomerated powder.

Acknowledgement

The authors would like to thank the financial support from China Scholarship Council (No.201606350091) and Teagasc project (0153).

Reference

Ahmed, M.R., McSweeney, S., Kruse, J., Vos, B., Fitzpatrick, D., (2018). Contactless, probeless and non-titrimetric determination of acid-base reactions using broadband acoustic resonance dissolution spectroscopy (BARDS). Analyst 143(4), 956-962.

Al hassn, A.Z., Jeßberger, S., Hounslow, M.J., Salman, A.D., (2018). Multi-stage granulation: An approach to enhance final granule attributes. Chemical Engineering Research and Design 134, 26-35.

Baldwin, A.J., (2010). Insolubility of milk powder products – A minireview. Dairy Science & Technology 90(2-3), 169-179.

Chever, S., Mejean, S., Dolivet, A., Mei, F., Den Boer, C.M., Le Barzic, G., Jeantet, R., Schuck, P., (2017). Agglomeration during spray drying: Physical and rehydration properties of whole milk/sugar mixture powders. Lwt-Food Science and Technology 83, 33-41.

Crawford, F.S., (1982). The hot chocolate effect. American Journal of Physics 50(5), 7.

Crowley, S.V., Desautel, B., Gazi, I., Kelly, A.L., Huppertz, T., O'Mahony, J.A., (2015). Rehydration characteristics of milk protein concentrate powders. Journal of Food Engineering 149, 105-113.

Felix da Silva, D., Ahrné, L., Ipsen, R., Hougaard, A.B., (2018). Casein-Based Powders: Characteristics and Rehydration Properties. Comprehensive Reviews in Food Science and Food Safety 17(1), 240-254.

Fitzpatrick, D., Evans-Hurson, R., Fu, Y., Burke, T., Kruse, J., Vos, B., McSweeney, S.G., Casaubieilh, P., Keating, J.J., (2014). Rapid profiling of enteric coated drug delivery spheres via broadband acoustic resonance dissolution spectroscopy (BARDS). Analyst 139(5), 1000-1006.

Fitzpatrick, D., Kruse, J., Vos, B., Foley, O., Gleeson, D., O'Gorman, E., O'Keefe, R., (2012). Principles and applications of broadband acoustic resonance dissolution spectroscopy (BARDS): a sound approach for the analysis of compounds. Anal Chem 84(5), 2202-2210.

Fitzpatrick, J.J., van Lauwe, A., Coursol, M., O'Brien, A., Fitzpatrick, K.L., Ji, J.J., Miao, S., (2016). Investigation of the rehydration behaviour of food powders by comparing the behaviour of twelve powders with different properties. Powder Technology 297, 340-348.

Foerster, M., Gengenbach, T., Woo, M.W., Selomulya, C., (2016a). The impact of atomization on the surface composition of spray-dried milk droplets. Colloids Surf B Biointerfaces 140, 460-471.

Foerster, M., Gengenbach, T., Woo, M.W., Selomulya, C., (2016b). The influence of the chemical surface composition on the drying process of milk droplets. Advanced Powder Technology 27(6), 2324-2334.

Fu, N., Woo, M.W., Selomulya, C., Chen, X.D., (2013). Shrinkage behaviour of skim milk droplets during air drying. Journal of Food Engineering 116(1), 37-44.

Gaiani, C., Banon, S., Scher, J., Schuck, P., Hardy, J., (2005). Use of a turbidity sensor to characterize micellar casein powder rehydration: Influence of some technological effects. Journal of Dairy Science 88(8), 2700-2706.

Ji, J.F., Cronin, K., Fitzpatrick, J., Fenelon, M., Miao, S., (2015). Effects of fluid bed agglomeration on the structure modification and reconstitution behaviour of milk protein isolate powders. Journal of Food Engineering 167, 175-182.

Jinapong, N., Suphantharika, M., Jamnong, P., (2008). Production of instant soymilk powders by ultrafiltration, spray drying and fluidized bed agglomeration. Journal of Food Engineering 84(2), 194-205.

Li, K., Woo, M.W., Selomulya, C., (2016). Effects of composition and relative humidity on the functional and storage properties of spray dried model milk emulsions. Journal of Food Engineering 169, 196-204.

Mimouni, A., Deeth, H.C., Whittaker, A.K., Gidley, M.J., Bhandari, B.R., (2010). Investigation of the microstructure of milk protein concentrate powders during rehydration: alterations during storage. J Dairy Sci 93(2), 463-472.

Niro, G., (2006). A11a-Particle density, occluded air and interstitial air by air pycnometer. GEA Process Engineering A/S, Gladsaxevej, Denmark.

Peddapatla, R.V.G., Ahmed, M.R., Blackshields, C.A., Sousa-Gallagher, M.J., McSweeney, S., Kruse, J., Crean, A.M., Fitzpatrick, D., (2017). Broadband Acoustic Resonance Dissolution Spectroscopy (BARDS) - A novel approach to investigate the wettability of pharmaceutical powder blends. Mol Pharm.

Schuck, P., (2009). *Dairy-derived ingredients*. Woodhead Publishing Limited.

400 Szulc, K., Lenart, A., (2013). Surface modification of dairy powders: Effects of fluid-bed
401 agglomeration and coating. International Dairy Journal 33(1), 55-61.
402 Vos, B., Crowley, S.V., O'Sullivan, J., Evans-Hurson, R., McSweeney, S., Krüse, J., Rizwan Ahmed, M.,
403 Fitzpatrick, D., O'Mahony, J.A., (2016). New insights into the mechanism of rehydration of milk
404 protein concentrate powders determined by Broadband Acoustic Resonance Dissolution
405 Spectroscopy (BARDS). Food Hydrocolloids 61, 933-945.
406 Wu, S., Fitzpatrick, J., Cronin, K., Miao, S., (2019). The effect of pH on the wetting and dissolution of
407 milk protein isolate powder. Journal of Food Engineering 240, 114-119.

Table 1
Particle size of MPI and MPI agglomerates.

Sample	MPI	MPI-W1	MPI-W2	MPI-L1	MPI-L2
D[V, 0.1] / μm	22.6±1.4[a]	47.7±2.0[b]	69.3±9.3[c]	53.0±0.7[b]	71.2±2.2[c]
D[V, 0.5] / μm	49.8±2.5[a]	118.8±1.7[b]	207.3±15.5[d]	117.3±3.5[b]	168.8±9.3[c]
D[V, 0.9] / μm	95.6±2.1[a]	193.0±2.3[b]	334.7±20.0[d]	189.8±9.3[b]	290.2±14.6[c]

Table 2
Densities and porosity of MPI and MPI agglomerates.

	MPI	MPI-W1	MPI-W2	MPI-L1	MPI-L2
Loose bulk density (g/L)	261±2	226±6	223±18	218±4	200±6
Tapped bulk density (g/L)	431±5	330±6	277±4	311±0	265±1
Apparent density (g/L)	1073±83	1119±22	1108±39	1103±5	1082±31
Porosity %	59.5± 0.42	70.5± 0.49	75.0± 0.37	71.8± 0.04	75.5± 0.06

Table 3
Specific air volumes of MPI and MPI agglomerates: bulk interstitial air, tapped occluded air, vacuole occluded air.

	Unit	MPI	MPI-W1	MPI-W2	MPI-L1	MPI-L2
Bulk interstitial air	mL/ 100g	151±0[b]	140±16[b]	89±22[a]	139±9[b]	122±16[ab]
Tapped occluded air	mL/ 100g	139±2[a]	214±5[b]	271±5[d]	230±0[c]	284±1[e]
Vacuole occluded air	mL/ 100g	27.8±1.0[c]	24.0±0.3[a]	24.8±0.4[ab]	25.7±0[b]	27.5±0.4[c]

Table 4
Time (t_M) at frequency minimum (or gas volume maximum) during BARDS test for MPI and MPI agglomerates.

Concentration (w/v)	Components	t_M (s)
0.10 %	MPI	140
	MPI-W1	109
	MPI-W2	85
	MPI-L1	80
	MPI-L2	60
0.15 %	MPI	140
	MPI-W1	118
	MPI-W2	109
	MPI-L1	93
	MPI-L2	80
0.20 %	MPI	244
	MPI-W1	163
	MPI-W2	118
	MPI-L1	101
	MPI-L2	80

FIGURES

List of Figures

Fig.1. Illustration of air in agglomerated MPI powder: vacuole occluded air within primary MPI particles, occluded air between primary particles within agglomerates, and tapped interstitial air between agglomerates.

Fig.2. A representative spectrum of 0.025 g agglomerated MPI in BARDS, showing different phases of the spectrum.

Fig.3. (A) BARDS frequency spectrum and (B) gas volume profile of MPI and MPI-W2 agglomerate at 0.1 % concentration.

Fig.4. The BARDS frequency spectrum for MPI, MPI-W, MPI-L at concentrations of A: 0.1 %, B: 0.15 %, C: 0.2 %.

Fig.5. The gas volume profile for MPI, MPI-W, MPI-L at concentrations of A: 0.1 %, B: 0.15 %, C: 0.2 %.

Fig.1

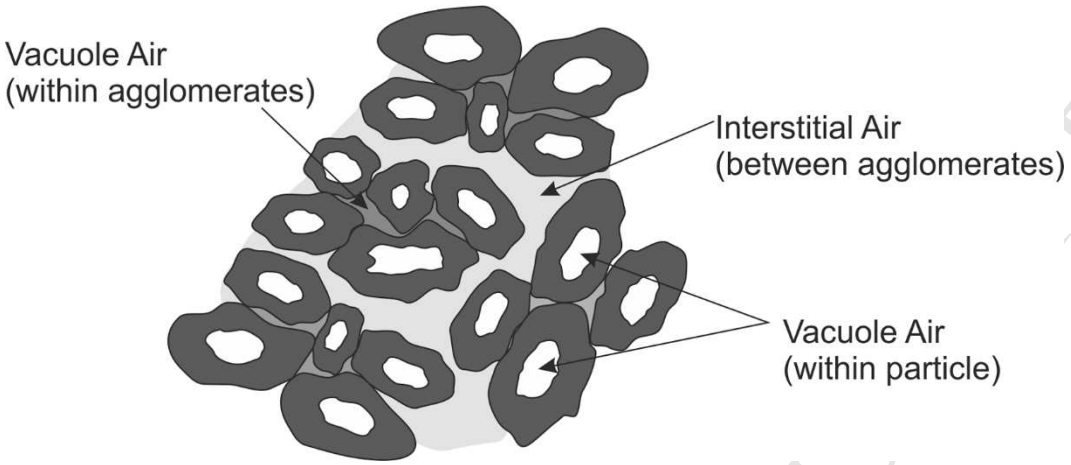

Fig.1. Illustration of air in agglomerated MPI powder: vacuole occluded air within primary MPI particles, occluded air between primary particles within agglomerates, and tapped interstitial air between agglomerates.

Fig.2

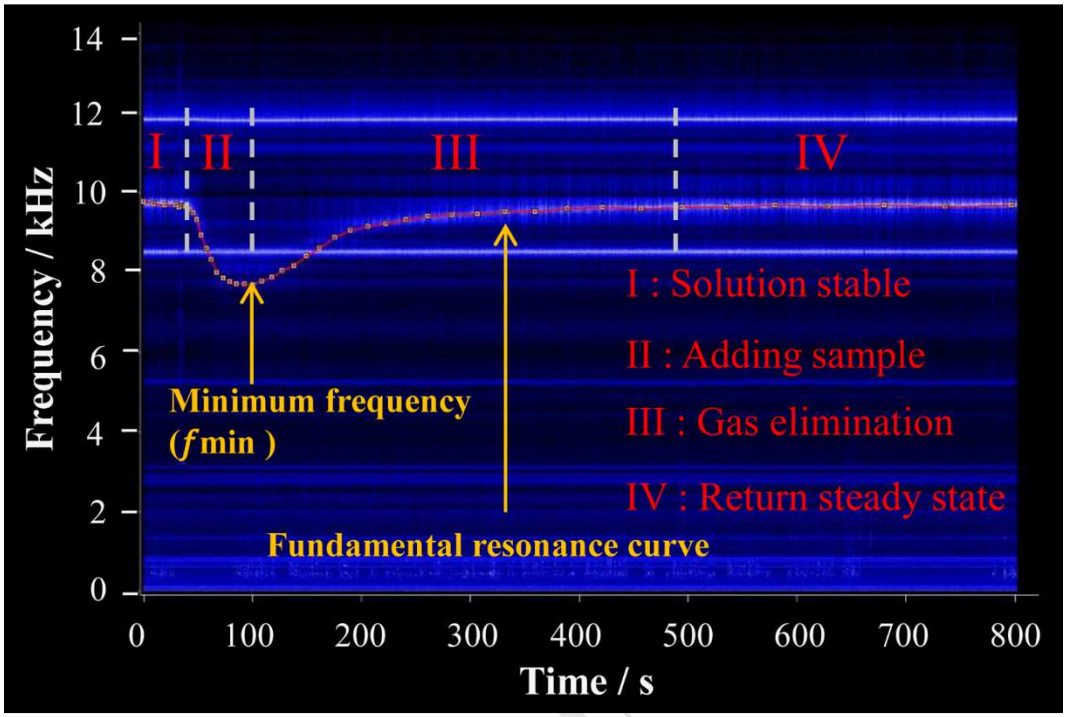

Fig.2. A representative spectrum of 0.025 g agglomerated MPI in BARDS, showing different phases of the spectrum.

Fig.3

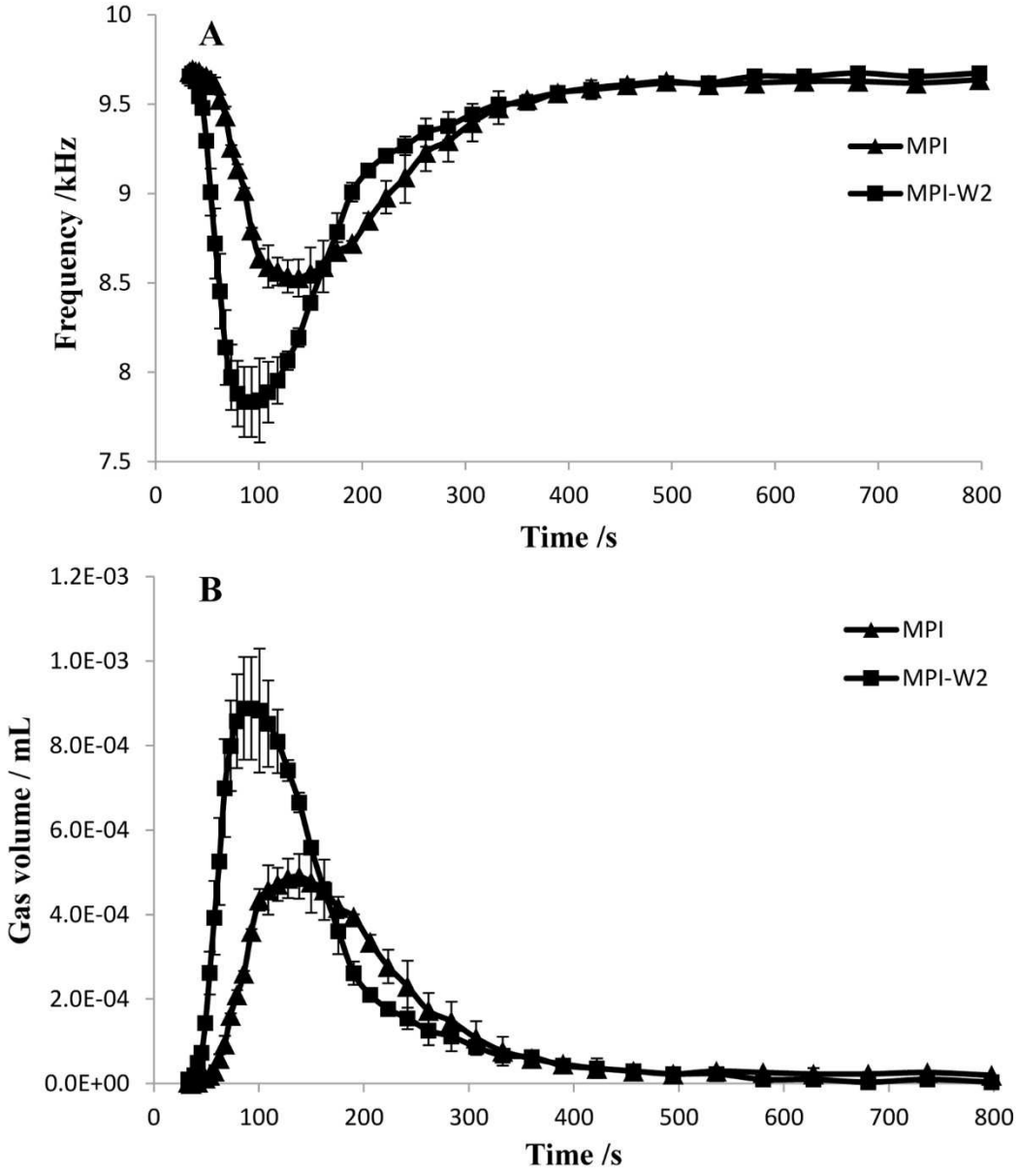

Fig.3. (A) BARDS frequency spectrum and (B) gas volume profile of MPI and MPI-W2 agglomerate at 0.1 % concentration.

Fig.4

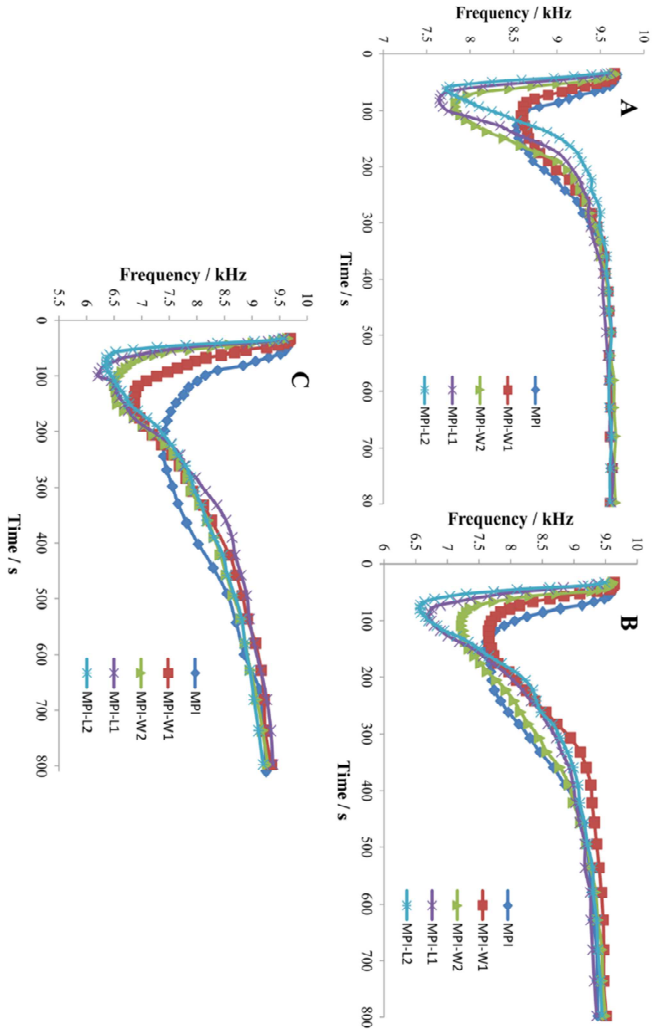

Fig.4. The BARDS frequency spectrum for MPI, MPI-W, MPI-L at concentrations of A: 0.1 %, B: 0.15 %, C: 0.2 %.

Fig.5

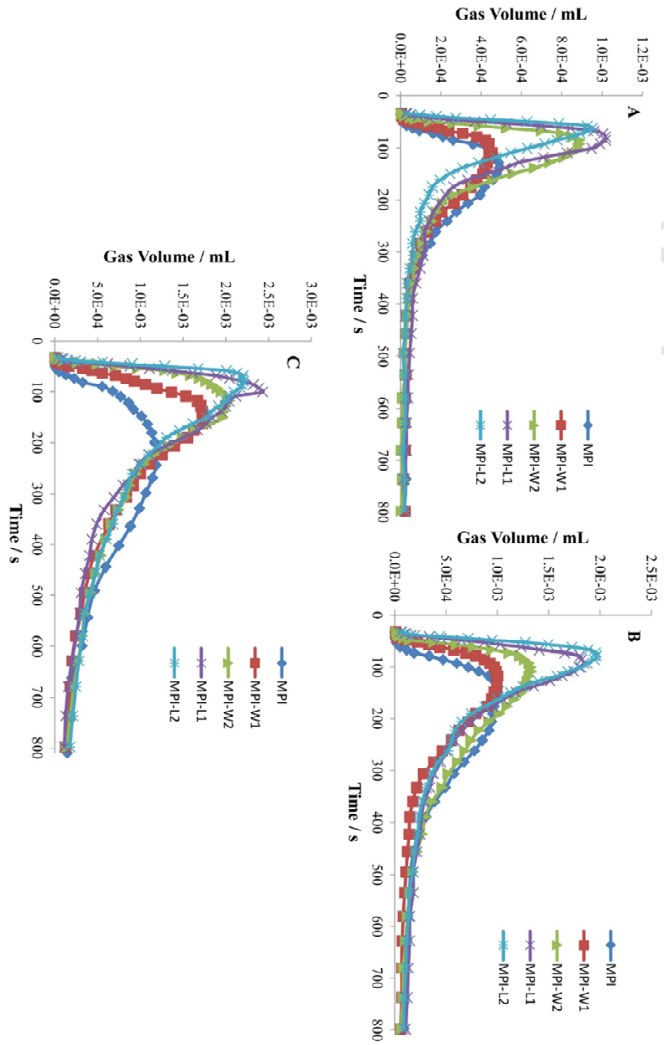

Fig.5. The gas volume profile for MPI, MPI-W, MPI-L at concentrations of A: 0.1 %, B: 0.15 %, C: 0.2 %.

Highlights:

1. BARDS successfully monitored rehydration of MPI agglomerates.

2. BARDS showed that MPI agglomerates wetted more quickly than MPI powder.

3. BARDS showed that agglomerate size and binder type influenced rehydration.

4. Dissolution of MPI agglomerates was rate-limited by dissolution of primary MPI particles.